JARO 19: 363–379 (2018)
DOI: 10.1007/s10162-018-0670-z

Research Article

JARO
Journal of the Association for Research in Otolaryngology

Platelet-Derived Growth Factor Subunit B Signaling Promotes Pericyte Migration in Response to Loud Sound in the Cochlear Stria Vascularis

Zhiqiang Hou,[1] Xiaohan Wang,[1] Jing Cai,[1] Jinhui Zhang,[1] Ahmed Hassan,[2] Manfred Auer,[3] and Xiaorui Shi[1]

[1]*Oregon Hearing Research Center, Department of Otolaryngology/Head & Neck Surgery, Oregon Health & Science University, Portland, OR 97239, USA*

[2]*Department of Biomedical Engineering, The University of Texas at Austin, Austin, TX 78712, USA*

[3]*Life Sciences Division, Lawrence Berkeley National Laboratory, Berkeley, CA 94720, USA*

Received: 15 December 2017; Accepted: 19 April 2018; Online publication: 4 June 2018

ABSTRACT

Normal blood supply to the cochlea is critical for hearing. Noise damages auditory sensory cells and has a marked effect on the microvasculature in the cochlear lateral wall. Pericytes in the stria vascularis (strial pericytes) are particularly vulnerable and sensitive to acoustic trauma. Exposure of NG2DsRedBAC transgenic mice (6–8 weeks old) to wide-band noise at a level of 120 dB for 3 h per day for 2 consecutive days produced a significant hearing threshold shift and caused pericytes to protrude and migrate from their normal endothelial attachment sites. The pericyte migration was associated with increased expression of platelet-derived growth factor beta (PDGF-BB). Blockade of PDGF-BB signaling with either imatinib, a potent PDGF-BB receptor (PDGFR) inhibitor, or APB5, a specific PDGFRβ blocker, significantly attenuated the pericyte migration from strial vessel walls. The PDGF-BB-mediated strial pericyte migration was further confirmed in an *in vitro* cell migration assay, as well as in an *in vivo* live animal model used in conjunction with confocal fluorescence microscopy. Pericyte migration took one of two different forms, here denoted protrusion and detachment. The protrusion is characterized by pericytes with a prominent triangular shape, or pericytes extending fine strands to neighboring capillaries. The detachment is characterized by pericyte detachment and movement away from vessels. We also found the sites of pericyte migration highly associated with regions of vascular leakage. In particular, under transmission electron microscopy (TEM), multiple vesicles at the sites of endothelial cells with loosely attached pericytes were observed. These data show that cochlear pericytes are markedly affected by acoustic trauma, causing them to display abnormal morphology. The effect of loud sound on pericytes is mediated by upregulation of PDGF-BB. Normal functioning pericytes are required for vascular stability.

Keywords: mouse cochlea, loud sound, pericyte, stria vascularis

INTRODUCTION

Pericytes are specialized mural cells located on the abluminal surface of microvessels. They are critical for vascular development, regulation of blood flow, vascular integrity, angiogenesis, and tissue fibrogenesis (Dore-Duffy et al. 2006; Peppiatt et al. 2006; Quaegebeur et al. 2010; Greenhalgh et al. 2013; Hall et al. 2014). Pericyte pathology leads to vascular

Zhiqiang Hou and Xiaohan Wang contributed equally to this work.

Correspondence to: Xiaorui Shi · Oregon Hearing Research Center, Department of Otolaryngology/Head & Neck Surgery · Oregon Health & Science University · Portland, OR 97239, USA. email: shix@ohsu.edu

dysfunction, such as seen in brain stroke, heart infarct, and retinal disease (Liu et al. 2012; Greif and Eichmann 2014; O'Farrell and Attwell 2014; Greenhalgh et al. 2015), and diabetic retinopathy (Pfister et al. 2008; Kim et al. 2016).

Normal function of the cochlear microvasculature is critical for maintaining the endocochlear potential (EP), ion transport, and fluid balance (Salt et al. 1987; Gratton et al. 1996; Wangemann 2002; Cohen-Salmon et al. 2007; Ohlemiller et al. 2008; Shi 2011; Chen et al. 2014b; Ingham et al. 2016). A reduction in blood flow to the cochlea leads to a shortage of nutrients and oxygen in the tissue and creates a "toxic" environment with accumulation of harmful metabolites. A unique feature of strial blood vessels is that they contain a rich population of pericytes, as illustrated in Fig. 1(A). The pericytes interact with endothelium to constitute a unique intrastrial fluid-blood barrier in the stria vascularis (Shi 2016). The structural integrity of the intrastrial fluid-blood barrier in the stria vascularis is essential for hearing (Salt et al. 1987; Gratton et al. 1996; Choudhury et al. 2009; Dai and Shi 2011; Shi 2011; Neng et al. 2013; Shi 2016).

The role of strial pericytes in normal hearing and hearing disorders is unknown. In general, a high density of pericytes in a region is often indicative of particularly important physiology in the area (Sims 1986). Pericyte pathology in the region would have a significant adverse effect on the regional vascular function. Our initial studies on cochlear pericytes showed that the pericytes in the stria vascularis are critical for maintaining the tightness of the intrastrial fluid-blood barrier (Neng et al. 2013). Recently, we found strial pericytes are responsive and vulnerable to changes in environmental conditions such as aging and inflammation. Strial pericyte initiated release of vesicles and pericyte migration is found both in aged animals (Neng et al. 2015) and under inflammatory conditions (Zhang et al. 2015). In this study, we have further demonstrated the vulnerability of strial pericytes and strikingly changes in pericyte morphology in response to loud sound. Pericyte protrusion and detachment from vessel walls are seen in different regions of the stria vascularis following exposure to long duration loud sound. The underlying mechanisms of these changes in pericytes are not yet known.

Pericyte migration has also been seen in the brain (Dore-Duffy et al. 2000), retina (Chen et al. 2011), and heart (O'Farrell and Attwell 2014) in response to stress and injury. Researchers have found pericyte migration is an early sign of brain hypoxia (Gonul et al. 2002) and indicative of severe pathology in diabetic retinopathy (Pfister et al. 2008; Kim et al. 2016). Cell migration is a typical response to environmental stimuli in addition to secretion of growth factors and cytokines (Devreotes and Horwitz 2015). The signals and mechanisms governing pericyte migration are not yet fully established. In this study, we identified PDGF-BB, a mitogenic growth factor, as a trigger for pericyte migration in the inner ear.

PDGF belongs to a family of four chain (A–D) growth factors essential for many key cellular processes in mesenchymal cells (Donovan et al. 2013). In particular, PDGF-BB binds its receptor PDGFRβ to activate downstream signaling pathways to regulate pericyte survival, migration, apoptosis, proliferation, and differentiation. Studies have shown that PDGF-BB/PDGFRβ activates Ras/Rho/Rac and protein kinase C signaling, leading to pericyte dissociation from abluminal endothelial surfaces and inducing protrusion of cellular processes away from vessels (Aguilera and Brekken 2014).

Strial tissue edema and vascular leakage are known as the consequences of acoustic trauma. However, it has not been known whether pericyte migration accompanies these pathological outcomes. In this report, we used a fluorescent reporter transgenic mouse model (NG2DsRed transgenic mice) to track both pericyte migration and non-pericyte migration-related vascular pathological consequences. We particularly focus on vascular permeability. We found that loud sound-induced vascular leakage occurs predominantly at sites of pericyte migration. The findings imply that pericyte migration may be a causal pathogenic event contributing to strial edema following loud sound trauma in the auditory system. The results suggest targeting of pericyte migration may provide opportunities for new therapies for preventing early noise-induced tissue swelling and edema. A better ion microenvironment could give injured sensory hair cells a better chance to survive by increasing cochlear oxygenation, potentially facilitating hearing recovery.

MATERIALS AND METHODS

Animals

NG2DsRedBAC transgenic (008241, 6–8 weeks old) and C57BL/6J (000664, 6–8 weeks old) strains of mice were purchased from Jackson Laboratory (Bar Harbor, Me., USA). All procedures in this study were reviewed and approved by the Institutional Animal Care and Use Committee (IACUC) at Oregon Health & Science University (IP 00000968).

Loud Sound Exposure

Animals with a positive Preyer reflex were divided into control and loud sound-stimulated groups. Animals receiving loud sound exposure were placed in wire mesh cages and exposed to broadband noise at

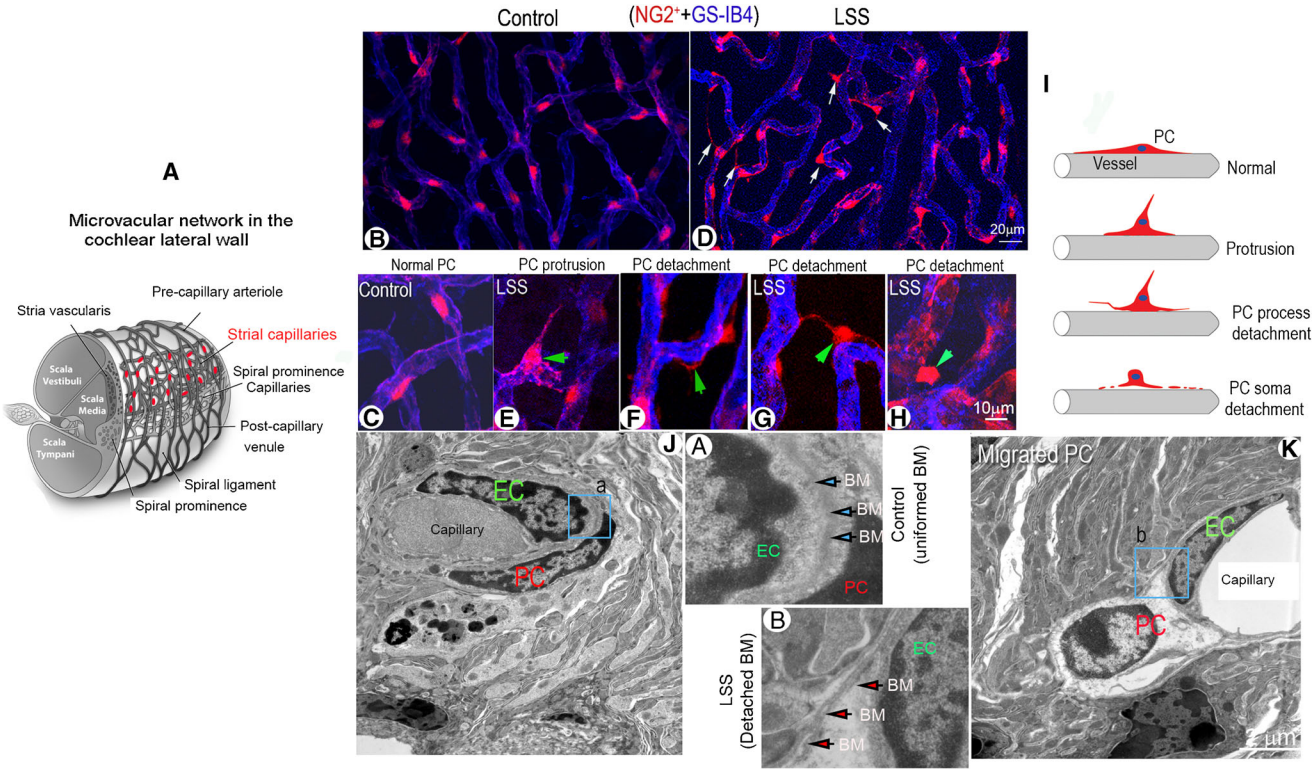

FIG. 1. Acoustic trauma causes strial pericyte protrusion and migration. (A) Schematic overview of cochlear blood supply in the cochlear lateral wall. The capillaries of the stria vascularis contain a rich population of pericytes. (B and C) Confocal low magnification images show pericyte distribution and morphology in control and loud sound-stimulated cochleae from fluorescent reporter mice ($NG2^+$, red). (B, C) Pericytes are shown with a flat body and evenly distributed on strial vessel walls (labeled with GS-IB4, blue) under normal conditions under low and high magnification. (D) Pericyte protrusion and detachment is seen under loud sound-stimulated conditions (white arrows). (E, F, G, H) are high magnification confocal projection images showing a range of different patterns in pericyte migration under loud sound-stimulated conditions. (F) shows a pericyte process detaching from the capillary wall in a loud sound-stimulated mouse (green arrow). (E, G) show pericytes sending fine strands to neighboring pericytes (green arrow). (H) shows retraction of a pericyte away from the capillary wall (green arrow). (I) The schematic figure illustrates the variety of patterns of pericyte detachment. (J) In this TEM image, a pericyte is shown closely associated with an endothelial cell in a control mouse cochlea. (K) shows a pericyte soma dissociated from the capillary wall in a loud sound-stimulated mouse cochlea. (a and b) are close-up images respectively from regions of (a) and (b) in panels (J) and (K) showing the structure of the basement membrane under control and LSS conditions. (LSS: loud sound stimulation, EC: endothelial cell, PC: pericyte, BM: basement membrane)

120 dB sound pressure level (A-weighted, SPL) in a sound exposure booth for 3 h and an additional 3 h the next day. This regime of intense sound exposure, routinely used in our laboratory, produces permanent loss of cochlear sensitivity at all frequencies measured (4, 8, 16, 24, and 32 kHz)(Shi 2009; Zhang et al. 2013).

Quantitative Real-Time Polymerase Chain Reaction

mRNA expression of *PDGF-BB* in the stria vascularis of control and loud sound-stimulated groups was measured by quantitative real-time PCR. Total RNA was extracted with an RNeasy kit (74204, Qiagen, Valencia, CA) from control and loud sound-stimulated groups (cohorts of 3 mice). Two micrograms of total RNA sample was reverse-transcribed using a RETROscript kit (AM1710, Ambion, Austin, TX, USA). The cDNA synthesized from total RNA was diluted 10-fold with DNase-free water. Transcript quantities were assayed by TaqMan gene expression assay for *PDGF-BB* (4331182, mouse, amplicon length 61, Mm00440678_m1, size 75 rxn. padded amplicon for Mm00440678_m1: accacctcgc ctgcaagtgt gagacagtag tgacccctcg gcctgtgact agaagtcctg ggacatccag ggagcagcga gccaagacgc ctcaagctcg ggtgaccatt cggacggtga gaatccgccg gccccccaaa ggcaagcacc gaaagtttaa) with a StepOnePlus real-time PCR system (Applied Biosystems, CA, USA). Thermal cycling conditions were 95 °C for 20 s, 40 cycles of 95 °C for 1 s, 60 °C for 20 s. Mouse Gapdh (4352339E, Applied Biosystems, CA, USA) expression was the endogenous control. Samples were run in triplicate for *PDGF-BB*. Quantitative PCR was performed according to the guidelines provided by Applied Biosystems. The comparative cycle threshold

(C_T) method ($\Delta\Delta C_T$ quantitation) was used to calculate the difference between samples.

ELISA and Western Blot Analysis

Protein level of PDGF-BB in the stria vascularis of control and loud sound-stimulated groups was measured by both ELISA and Western blot. For the ELISA measurement, 12 samples of whole mounts of stria vascularis from 4 control and 4 loud sound-stimulated animals were assessed. The level of PDGF-BB is estimated with an enzyme-linked immunosorbent assay (ELISA) kit (catalog no. MBB00; R&D Systems, Minneapolis, MN, USA) used per company instructions. The fluorescence signals were detected with a Tecan GENios Plus microplate reader at an excitation wavelength of 450 nm, with emission acquired through a 560-nm filter. The fluorescence signal reflects the level of PDGF-BB concentration. For western blot, 10 strial strips were isolated from 5 animals in each group and homogenized in lysis buffer cocktail with a protease inhibitor for 30 s. A total of 50 μg protein from each cohort was added to a 10 % sodium dodecyl sulfate–polyacrylamide gel for detection of PDGF-BB and GAPDH. Proteins were electrophoretically transferred to PVDF membranes and blocked with nonfat milk for 1 h at room temperature. Specific immunodetection was carried out by incubation with primary antibodies, with the anti-PDGF-BB antibody diluted 1:1000 in skim milk overnight at 4 °C. After 3 washes with TBST, the membranes were incubated for 1 h with secondary antibody, and antigens assessed using ECL Plus Western Blotting Detection Reagents (Amersham, Arlington Heights, IL, USA). WB analysis of PDGF-BB was performed to compare expression of PDGF-BB against the GAPDH endogenous control. Related antibody information is listed in Table 1.

Immunohistochemistry and Confocal Microscopy

Immunohistochemistry was previously reported by Zhang et al. (2012). Briefly, mice were deeply anesthetized with ketamine hydrochloride and xylazine hydrochloride as previously described. The mice were perfused intravascularly through the left ventricle with 1× phosphate-buffered saline (PBS, pH 7.4) to flush out circulating blood, followed by 4 % paraformaldehyde fixative. The mice were decapitated, the cochleae harvested and fixed in 4 % paraformaldehyde overnight. Whole-mounts of stria vascularis from different experiment groups were carefully isolated, after a wash in 1 × PBS, permeabilized in 0.5 % Triton X-100 (T8787, Sigma-Aldrich, USA) in 1× PBS for 0.5 h, and immuno-blocked with a solution of 1 % fish gelatin (G7765, Sigma-Aldrich, USA) in 1× PBS for an additional hour. The specimens were incubated overnight at 4 °C with a monoclonal primary antibody, rabbit anti-desmin (ab32362; Abcam, Cambridge, MA) in 1 % bovine serum albumin (BSA) in 1× PBS. After three washes in 1 × PBS, samples were incubated with the secondary antibody, Alexa Fluor 488-conjugated goat anti-rabbit IgG (A11008, Invitrogen Eugene, OR, USA) for 1 h at room temperature. Capillaries were labeled with the lectin Griffonia simplicifolia IB4 (GS-IB4) conjugated to Alexa Fluor 647 (I32450, Thermo Fisher Scientific, USA). The tissues were washed three times and mounted (H-1500, Vector Laboratories, USA). Controls were prepared by replacing primary antibodies with overnight incubation in PBS–BSA. The pericyte soma was identified by the red fluorescence emission of DsRed.T1 under the control of the mouse NG2 (*Cspg4*). Pericyte processes were identified by the green fluorescence emission of Alexa Fluor 488. The strial capillaries were visualized by the blue fluorescence emission of Alexa Fluro 647. In this study, pericyte migration was classified as either protrusion or detachment. Protrusion migration displays with the morphological change in pericytes from a normal flat cellular body to a prominent round body or triangular cell body with a fine strand at the top that is frequently connected to a neighboring vessel. This type of pericyte migration was described by Pfister et al. (2008). Detachment migration displays with movement of the pericyte soma or processes away from the capillary wall or movement away from the capillary. All images were acquired by confocal microscopy (Olympus FV1000, Japan), saved as OIB files, and processed using Adobe Photoshop CS2 (Adobe Systems, San Jose, CA, USA). Adobe Photoshop was used to merge and combine multiple images.

To detect PDGFR-β protein expression in migrated and non-migrated pericytes, a fluorescence lectin dye (DL-1178, Vector, 50 mg/ml, 100 μl) was administrated through the retro-orbital sinus to label blood vessels for 5 min before animals were sacrificed. Whole-mounts of the stria vascularis from control and loud sound-stimulated animals were then isolated and fixed. The specimens were incubated overnight at 4 °C with a primary antibody for PDGFR-β (ab32570; Abcam, Cambridge, MA) in 1 % bovine serum albumin (BSA) in 1× PBS. After three washes in 1 × PBS, samples were incubated with the secondary antibody, Alexa Fluor 488-conjugated goat anti-rabbit IgG (A11008, Invitrogen Eugene, OR), for 1 h at room temperature. All images were acquired by confocal microscopy (Olympus FV1000, Japan), saved as OIB files, and processed using Adobe Photoshop CS2 (Adobe Systems, San Jose, CA, USA). To determine fluorescence intensity of the PDGFR-β protein

TABLE 1

Antibodies applied in the study

Antibodies	*Vendors*	*Catalog number*	*Dilution*	*Source*	*Specificity*
PDGFR β	Abcam, Cambridge, MA	ab32570	1:50(with 1 % BSA-PBS)	Rabbit	Mouse, rat, human
PDGF-BB	Abcam, Cambridge, MA	ab181341	1:50 (with 1 % BSA-PBS)	Rabbit	Mouse, rat, human
Desmin	Abcam, Cambridge, MA	ab32362	1:50 (with 1 % BSA-PBS)	Rabbit	Mouse, rat, human
GAPDH	Santa Cruz Biotechnology	sc-20,357	1:200(with 1 % BSA-PBS)	Goat	Mouse, rat, human
Peroxidase-labeled anti-rabbit antibody	GE healthcare Bio-Sciences, Pittsburgh, PA	NIF 824	1:5000(with 5 % skim milk)	Donkey	Goat
Donkey anti-goat IgG-HRP	Santa Cruz Biotechnology, Dallas, TX	SC-2020	1:5000(with 5 % skim milk)	Donkey	Goat
Alexa Fluor 488-conjugated goat anti-rabbit IgG	Invitrogen, Eugene, OR	A-11008	1:100(with 1 % BSA-PBS)	Goat	Rabbit

expression, 20 relatively normal pericytes and 20 migrated pericytes from the same loud sound-stimulated tissues were selected and mean pixel values obtained using the ImageJ histogram analysis. Background intensity was determined from a small window located away from the fluorescence of the vessels and subtracted from the fluorescence intensity value of the cells. The mean value from each group was averaged for the 20 cells from 3 loud sound-stimulated tissues.

Transwell Migration Assay

An *in vitro* cell migration assay was used to determine if the PDDF-BB signal induces pericyte migration. Briefly, primary cultured strial pericytes at a concentration of 0.8×10^6 cells/ml were placed in upper compartments of a Boyden chamber (CBA-100-C, CytoSelect™ Cell Migration Assay, Cell Biolabs, Inc., San Diego, CA, USA) containing PDGF-BB at 2, 4, or 8 ng/ml (P3201, Sigma-Aldrich, USA). The Boyden chambers were placed in an incubator for 6 h. Migrated pericytes passed through the polycarbonate membrane and attached to the bottom side. The non-migratory pericytes that remain in the upper insert are removed. Pericyte migration was assessed per instructions of the Cell Biolab manual. Each insert was transferred to a well containing 200 µl of lysis buffer and CyQuant® GR dye. Pericyte migration was evaluated by fluorometric analysis. Each concentration was tested at least 3 times. Fluorescence was recorded using a Tecan GENios Plus microplate reader at 450 nm excitation, 560 nm emission. The level of fluorescence signal reflects the degree of pericyte migration. The data were expressed as means ± S.D.

Pericyte Culture and Treatment

To investigate if PDGF-BB signals the pericyte migration, purified strial pericytes (Neng et al. 2013) at the third passage were divided into control and PDGF-BB-treated groups. Pericytes were plated in collagen-coated dishes at a density of 1×10^4 cells/dish. In the control group, pericytes were incubated in pericyte culture medium for 6 h, while in the PDGF-BB-treated group, the pericytes were exposed to pericyte culture medium containing PDGF-BB (P3201, Sigma-Aldrich, USA) at 2, 4, or 8 ng/ml for 6 h, respectively. At the end of the experiment, pericytes were fixed with 4 % paraformaldehyde for 15 min, permeabilized with 0.25 % triton for 30 min, and triple immunolabeled with antibody for desmin (1:100, ab32362, Abcam), Alexa Fluor® 647 phalloidin, a fluorescence dye for cellular cytoskeleton F-actin (1:100, A22287, Life Technologies, USA), and Hoechst, a fluorescence dye for cell nuclei (H-3569, 1:10000, Molecular Probes, USA). All images were taken using the same exposure time and laser intensity. Images were acquired with a × 10 objective under an FV1000 Olympus laser-scanning confocal microscope. A total of 20 images were recorded from each treatment group. Polarized pericytes were identified by their thin and long processes or unevenly distributed actin. Non-polarized pericytes were identified by their large, broad filopodia morphology, as described by Shepro and Morel (1993). For fluorescence measurements of F-actin and desmin expression, a series of images were obtained from control and PDGF-BB-treated groups. The fluorescence intensity of F-actin or desmin was measured as a mean value determined with the ImageJ histogram analysis. A background intensity was determined from a small window

located away from the fluorescence of the vessels and subtracted from the fluorescence intensity value of the cells. The mean value from each group was averaged for 20 images collected from 2 trials.

In Vivo Animal Model

Pericyte migration was tested in a live animal model (in vivo) in which an open vessel-window (cochlear fenestra) was created in the cochlear lateral wall as previously reported, see (Shi et al. 2014). The vessel-window was created at the apex-middle turn, approximately 1.25 mm from the apex. A physiological solution containing 10 ng/ml PDGF-BB was directly superfused to the vessel-window for 30–60 min. The cochlea was fixed, and the full-length of the cochlear stria vascularis was isolated and immunolabeled with an antibody for desmin, a protein richly expressed in pericyte projections. The whole mount was examined under an Olympus inverted microscope fitted with a Fluoview FV1000 confocal laser system. Pericyte somas were identified by the red fluorescence signal of the NG2DsRed excited at 559 nm, with the emission acquired through a 600-nm filter. Pericyte projections were visualized at 488 nm excitation, with the emission acquired through a 550-nm filter.

Drug Treatment

To determine whether PDGF-BB/PDGF-β signaling mediates strial pericyte migration in the loud sound-stimulated condition, PDGF-BB/PDGFR-β signal was first blocked with imatinib, a potent PDGFR receptor blocker (S2475, Selleckchem, USA). Specifically, NG2DsRedBAC transgenic mice were divided into 4 groups (6 animals per group): (1) control; (2) loud sound-stimulated; (3) loud sound-stimulated + imatinib-treated; (4) loud sound-stimulated + saline-treated. For the treatment groups, imatinib at 100 mg/kg was prepared with saline and administered as an acute, single-dose intraperitoneal injection 1 h prior to loud sound stimulation. A similar dose was given the second day 1 h prior to loud sound stimulation. Control animals received the same volume of saline on the same schedule. Animals in the control and loud sound-stimulated groups were sacrificed immediately at the end of the sound exposure regime. Whole-mounts of the stria vascularis from each group were carefully isolated and fixed. The capillaries in the stria vascularis were labeled with GS-IB4-AlexaFluor-647. The number of pericyte migrations was counted over the entire length of stria vascularis for the control, loud sound-stimulated, and loud sound-stimulated + imatinib-treatedgroups, and calculated as a percentage:

$$\frac{\text{total number of protruded and detached pericytes}}{\text{total number of pericytes}} \times 100.$$

Data were expressed as means ± S.D.

We also blocked the PDGF-BB/PDGFR-β signal with APB5, an antibody which specifically targets PDGFR-β (Sano et al. 2001; Sano et al. 2002; Hayashi et al. 2008). APB5 at 200 µg (in 100 µl saline) was given as an acute, single-dose intraperitoneal injection 1 h prior to loud sound exposure. The same dose was administered on the second day of loud sound stimulation, again 1 h prior to loud sound exposure. Control animals received the same volume of control rat IgG at the same concentration and on the same schedule. Animals either in the loud sound-stimulated + IgG-treated or loud sound-stimulated + APB5-treated groups were sacrificed immediately at the end of the sound exposure regime. Whole-mounts of stria vascularis from each group were carefully isolated and fixed. The role of PDGF-BB in initiating pericyte migration was assessed from comparison of migrated pericytes from loud sound-stimulated + control IgG-treated and loud sound-stimulated + APB5-treated. Images were acquired with a ×20 objective. The number of pericyte migrations, including protrusions and detachments, was counted at the different cochlear turns of the stria vascularis. A standard reference was used to define the range of cochlear turns (Lentz et al. 2013). A total of 72 images were recorded from 8 loud sound-stimulated + control IgG-treated mice and a total of 72 images from 8 loud sound-stimulated mice/APB 5-treated mice. Pericyte migration was calculated as a percentage:

$$\frac{\text{total number of protruded and detached pericytes}}{\text{total number of pericytes}} \times 100.$$

Data were expressed as means ± S.D.

Transmission Electron Microscopy

The temporal bones were isolated, and the cochlea perfused through the round window. This was followed by immersion in a fixative of 4 % (wt/vol) paraformaldehyde and 0.1 % (vol/vol) glutaraldehyde in 0.1 M phosphate-buffer overnight. Strial tissues were dissected and post fixed in 1 % osmium (Electron Microscopy Sciences, Hatfield, PA). Tissues were dehydrated with a graded alcohol series and embedded in Embed 812 (Electron Microscopy Sciences, Hatfield, PA), sectioned, stained with lead

citrate (Electron Microscopy Sciences, Hatfield, PA) and uranyl acetate (Electron Microscopy Sciences, Hatfield, PA), and viewed on a Philips CM 100 transmission electron microscope (Philips/FEI Corporation, Eindhoven, Holland).

Vascular Leakage Measurement

Pericyte migration-related vascular leakage was quantitatively analyzed by two experimental methods. In the first method, pericyte migration-related vascular barrier leakage was assessed by correlating the IgG fluorescence of tracer passed across capillary walls near the site of pericytes. Fluorescence tracer (Alexa Fluor® 488 conjugate goat anti-Human, MW = 150,000 Da, A-11013, Thermo Fisher Scientific) at 1.5 mg/ml in saline was intravenously administered to anesthetized animals in control and loud sound-stimulated groups for 30 min prior to harvesting, a method we previously published (Zhang et al. 2013). Circulating blood cells and administered IgG tracer were flushed by left ventricle perfusion with PBS from the animal cardiovascular system, and then the mice were decapitated. Whole mounts of the stria vascularis from both groups were isolated and fixed. The capillaries in the stria vascularis were labeled with isolectin GS-IB4-AlexaFluor-647. IgG leakage was assessed using confocal microscopy to evaluate Alexa Fluor-488 fluorescence signal outside capillary walls in the vicinity of NG2DsRed fluorescence labeled migrated- and non-migrated pericytes.

In the second method, pericyte migration-related vascular barrier leakage was assessed by correlating horseradish peroxidase (HRP) tracer outside capillary walls with the location of pericytes. Mice in control and loud sound-stimulated groups were anesthetized. Type II HRP (P8250, Sigma-Aldrich, USA) solution at 100 µl (50 mg/ml) was intravenously administrated to animals. Thirty minutes later, heart perfusion was performed with 1 × PBS (pH 7.4) to flush the circulating blood. Cochleae were isolated and fixed with phosphate-buffered 3 % glutaraldehyde and 1.5 % PFA for 5 h. Stria vascularis from control and loud sound-stimulated groups were isolated and incubated in reaction buffer (Pierce™ DAB Substrate Kit, 34002, Thermo Fisher Scientific, USA) containing DAB and stable peroxide substrate for 1 h. After chemical reaction, samples were post-fixed for 1 h in 1 % osmium. Tissues were dehydrated through a graded alcohol series, embedded in Embed 812 (Electron Microscopy Sciences, Hatfield, PA., USA), sectioned, stained for 2 min with UranyLess (Electron Microscopy Sciences, USA), and examined on an FEI Tecnai-12 BioTWIN transmission electron microscope.

Statistics and Analysis

Data were presented as means ± S.D and were compared using Student's t test for two groups or one-way ANOVA for three or more groups followed by a Tukey multiple comparison. $P < 0.05$ was considered statistically significant. SPSS 18.0 software was used for the statistical analysis.

RESULTS

Loud Sound Causes Pericyte Protrusion and Migration

In this study, we found that strial pericytes are highly vulnerable to acoustic trauma. We noticed the morphology of pericytes in the stria vascularis undergoes striking changes with loud sound exposure. In a normal mouse cochlea, strial pericytes on the vessel walls are oriented longitudinally and lie flat along the vessels, as shown in Fig. 1(B and C). However, when animals are exposed to wide-band loud sound at 120 dB, 3 h per day for 2 consecutive days, the pericytes become irregularly positioned along the vessel walls. A large number of the pericytes shed vesicles and begin to show protruding soma and detached processes, as shown in Fig. 1(D (white arrows)). Different patterns of pericyte migration are readily apparent under high magnification, as shown in Fig. 1(E–H (green arrows)).

We classified the pericyte migration as either "protrusion" or "detachment" based on displayed patterns. Protrusion is characterized by a morphological change in pericytes from their normal flat cellular body to a prominent round body (a protrusion or triangular cell body with a fine strand at the top that is frequently connected to a neighboring vessel), a sign of pericyte migration described by Pfister et al. 2008 and shown in Fig. 1(E and F). Detachment is characterized by dissociation from the strial capillary and movement of either the pericyte soma or pericyte process away from it, as shown in Fig. 1(G and H). Figure 1(I) is a schematic illustration of the different types of pericyte migration as a consequence of loud sound trauma.

At the ultrastructural level, a normal pericyte is closely associated with endothelial cells (ECs) and ensheathed by basement membrane (Fig. 1(J)). See the magnified image of panel (a) from region (a) of panel J. By contrast, a migrated pericyte is often dissociated from underlying ECs and displays with a disrupted basement membrane, as shown in Fig. 1(K). The magnified image of panel (b) from region (b) of panel K illustrates the dissociation.

Loud Sound Significantly Increases PDGF-BB Production in the Stria Vascularis, with the Migrated Pericytes Expressing High PDGF-BB Receptor

In this study, we found PDGF-BB, a potent mitogen and chemotactic factor (Facchiano et al. 2000), is significantly upregulated at both the transcriptional and protein level by the second day after loud sound exposure (Fig. 2). Figure 2(A) shows the increased level of *PDGF-BB* mRNA measured by quantitative real-time pericyte R analysis. PDGF-BB protein expression in the stria vascularis was also significantly elevated, measured by Western blot (Fig. 2(B and C)) and ELISA (Fig. 2(D)). Furthermore, immunohistochemical examination by confocal microscopy clearly showed PDGF-BB receptor, PDGFRβ, is increasingly expressed in the migrated pericytes. The expression was particularly conspicuous at these sites. Figure 2(E and F) is representative confocal maximum projection images showing immunofluorescent labeling of PDGFRβ (arrows, Fig. 2(F)). In contrast, the level of PDGFRβ expression in non-migrated pericytes was weak (arrows, Fig. 2(E)). Figure 2(G) shows the significant difference in fluorescence level for PDGFRβ expression in non-migrated pericytes and migrated pericytes.

Pericyte Migration Is Associated with Increased PDGF-BB Activity

To determine whether the PDGF-BB signal triggers pericyte migration, we first tested the hypothesis in an *in vitro* transwell migration assay. A schematic of the experiment is illustrated in Fig. 3(A). As expected, pericyte migration was markedly affected by PDGF-BB. Pericyte migration was significantly increased by PDGF-BB in a dose-dependent manner, as shown in Fig. 3(B). Dramatic changes in pericyte morphology were also seen associated with PDGF-BB dose, as shown in Fig. 3(C–F). Under control conditions, pericytes *in vitro* displayed a broad filopodia morphology (Fig. 3(C)), consistent with that previously described by Shepro and Morel (1993). In contrast, PDGF-BB-treated pericytes were thin with long processes (Fig. 3(D–F)). These features are better visualized under high magnification under control (Fig. 3(G)) and PDGF-BB-treated conditions (Fig. 3(H)). We also found significantly increased expression of cytoskeletal proteins such as F-actin and intermediate filament desmin when cells were treated with PDGF-BB (Fig. 3(J and K)).

To further corroborate PDGF-BB signaling-induced pericyte migration, we also conducted a study in an *in vivo* live animal model. We created a "vessel-window" (cochlear fenestra) over the cochlear lateral wall and directly applied PDGF-BB to the opened vessel-window approximately 1.25 mm from the apex (red box, Fig. 4(A)). After 30–60 topical minutes perfusion, the full-length of the cochlear stria vascularis was isolated, as shown in Fig. 4(B). The whole mounted stria vascularis was immunolabeled with desmin, a protein richly expressed in pericyte processes (Fig. 4(C)). We found pericytes in PDGF-BB-treated vessel-window areas to display prominent round bodied somas and detached foot processes. The foot processes were irregular and in less physical contact with endothelium, as shown in Fig. 4(E). In contrast, pericyte foot processes were closely associated with capillary walls in non-PDGF-BB-perfused areas, as shown in Fig. 4(D).

Blocking PDGF-BB Signaling Attenuates Pericyte Migration

We tested whether blocking PDDF-BB activity eliminates or attenuates loud sound-induced pericyte migration. Imatinib, a potent PDGFR blocker, was administered before loud sound stimulation. Control animals received the same volume of saline. We found that blocking the PDGF-BB signal significantly attenuated pericyte migration. The bar graph in Fig. 5 shows the significant change in pericyte migration between loud sound-stimulated and loud sound-stimulated/imatinib groups. In addition, we further confirmed the PDGF-BB signal is a trigger for pericyte migration by blocking the PDGF-BB signal with the neutralizing antibody (APB5). APB5 is a specific blocker for PDGFRβ (Sano et al. 2001; Sano et al. 2002; Hayashi et al. 2008). In this study, APB5 (200 μg) was given as an acute, single-dose intraperitoneal injection 1 h before loud sound stimulation. An identical dose was administered an hour before loud sound exposure on the second day. Control animals received the same amount of rat IgG at the same concentration and on the same schedule. We found the specific targeting of PDGFRβ reduced total pericyte migration from 21.8 ± 1.9 % in the loud sound-stimulated/control IgG-treated group to 9.7 ± 1.9 % in the loud sound-stimulated/APB5-treated group.

Regional Vascular Leakage Preferentially Occurs in Areas of Pericyte Migration

Pericytes in the strial capillary network sustain vascular integrity and stability. In the cochlea, vascular leakage and strial tissue edema are frequently seen following acoustic trauma (Yoshida and Liberman 1999; Suzuki et al. 2002; Armulik et al. 2010; Bell et al. 2010). However, it is not known whether pericyte migration initiates these changes, nor is it known whether vascular leakage primarily occurs at sites of pericyte migration. In this study, we compared vascular leakage in pericyte-migrated and non-

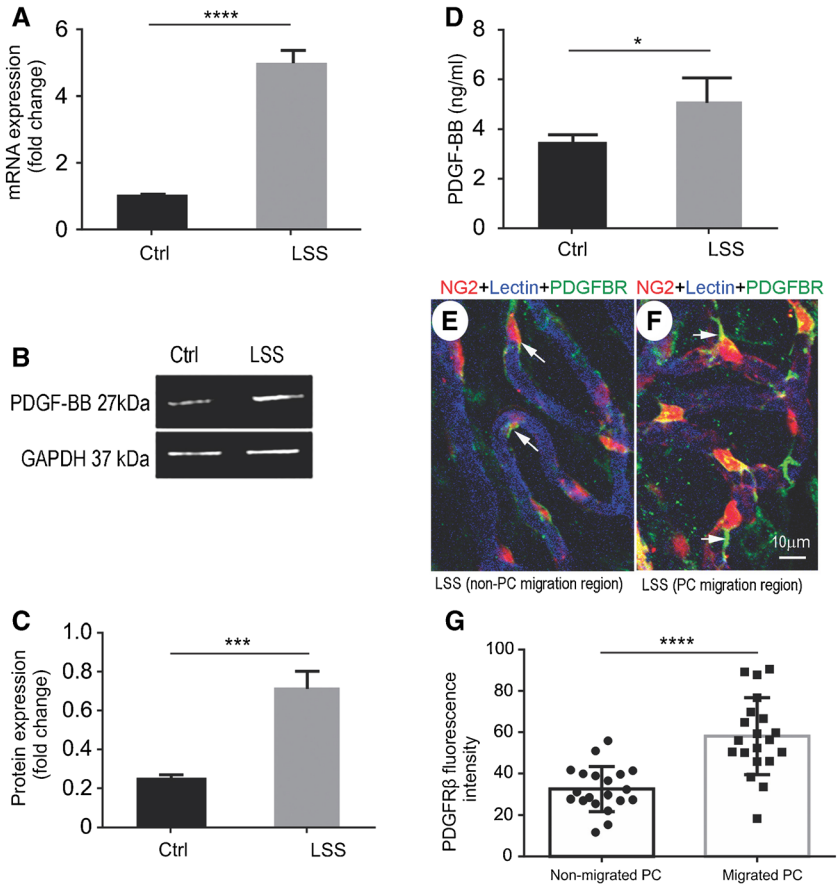

FIG. 2. Loud sound increases production of PDGF-BB in the stria vascularis, and migrated pericytes express higher PDGF-BB receptor (PDGFRβ). (A) The level of *PDGF-BB* mRNA is significantly increased after loud sound stimulation, measured by quantitative real-time pericyte [$n_{ctrl} = 3$, $n_{lss} = 3$, $t\,(4) = 17.63$, $^{****}P_{(\text{lss vs ctrl})} < 0.0001$, Student's t test]. (B, C) The level of PDGF-BB protein in the stria vascularis is also significantly elevated, measured by Western blot [$n_{ctrl} = 3$, $n_{lss} = 3$, $t\,(4) = 8.616$, $^{***}P_{(\text{lss vs ctrl})} = 0.001$, Student's t test]. (D) Increased production of PDGF-BB is also detected by ELISA [$n_{ctrl} = 4$, $n_{lss} = 4$, $t\,(4) = 3.121$, $^{*}P_{(\text{lss vs ctrl})} = 0.02 < 0.05$, Student's t test]. (E, F) The representative confocal projection images show PDGFRβ expression in non-migrated pericytes and migrated pericytes. (E) shows a relatively dim PDGFRβ fluorescence signal is detected in non-migrated pericytes (white arrows). (F) shows an increased fluorescence signal for PDGFRβ detected in the migrated-pericytes, particularly in the processes of migrated-pericytes (white arrows). (G), a bar graph, shows significantly higher fluorescence intensity for PDGFRβ in the migrated pericytes than non-migrated pericytes [$n_{non\text{-}migrated\ pc} = 20$, $n_{migrated\ pc} = 20$, $t\,(38) = 5.313$, $^{****}P_{(\text{non-migrated PC vs migrated PC})} < 0.0001$, Student's t test] (PC: pericyte)

pericyte-migrated regions of whole-mounted stria vascularis (Fig. 6(A and B)), and we found that circulating immunoglobulin G (IgG) extravasation was most apparent near areas of protruded pericyte (Fig. 6(B)). This pericyte protrusion is more evident in the magnified images of insert (a1) from panel A. Leaked IgG is also better visualized in insert b1 from panel B. The leakage is clearly demonstrated when capillaries are labeled with the fluorescence dye GS-IB4-Alexa Fluor-647 and imaged under high magnification, as shown in Fig. 6(C).

We also used horseradish peroxidase (HRP), an enzymatic tracer, in conjunction with transmission electron microscopy (TEM), to detail vascular leakage at the ultrastructural level. Figure 7 shows TEM micrographs of capillary profiles at non-pericyte-migrated and pericyte-migrated sites. HRP signal was virtually absent at non-pericyte-migrated sites after HRP was administrated in the blood circulation for 30 mins, as shown in Fig. 7(A). On the other hand, dark HRP signals were detected largely at sites of pericyte soma detachment. Figure 7(B) is a representative TEM image showing black HRP signals in the vicinity of a detached pericyte soma (indicated by the pink square area). These are better seen under high magnification in panel C (black arrows).

In addition, we noticed that the endothelial cell is flattened and its luminal surface smooth in non-migrated pericyte regions. A dense basement membrane embedding pericyte closely associates with endothelial cell (D, white arrow). In contrast, the luminal surface of the endothelial cell is undulated

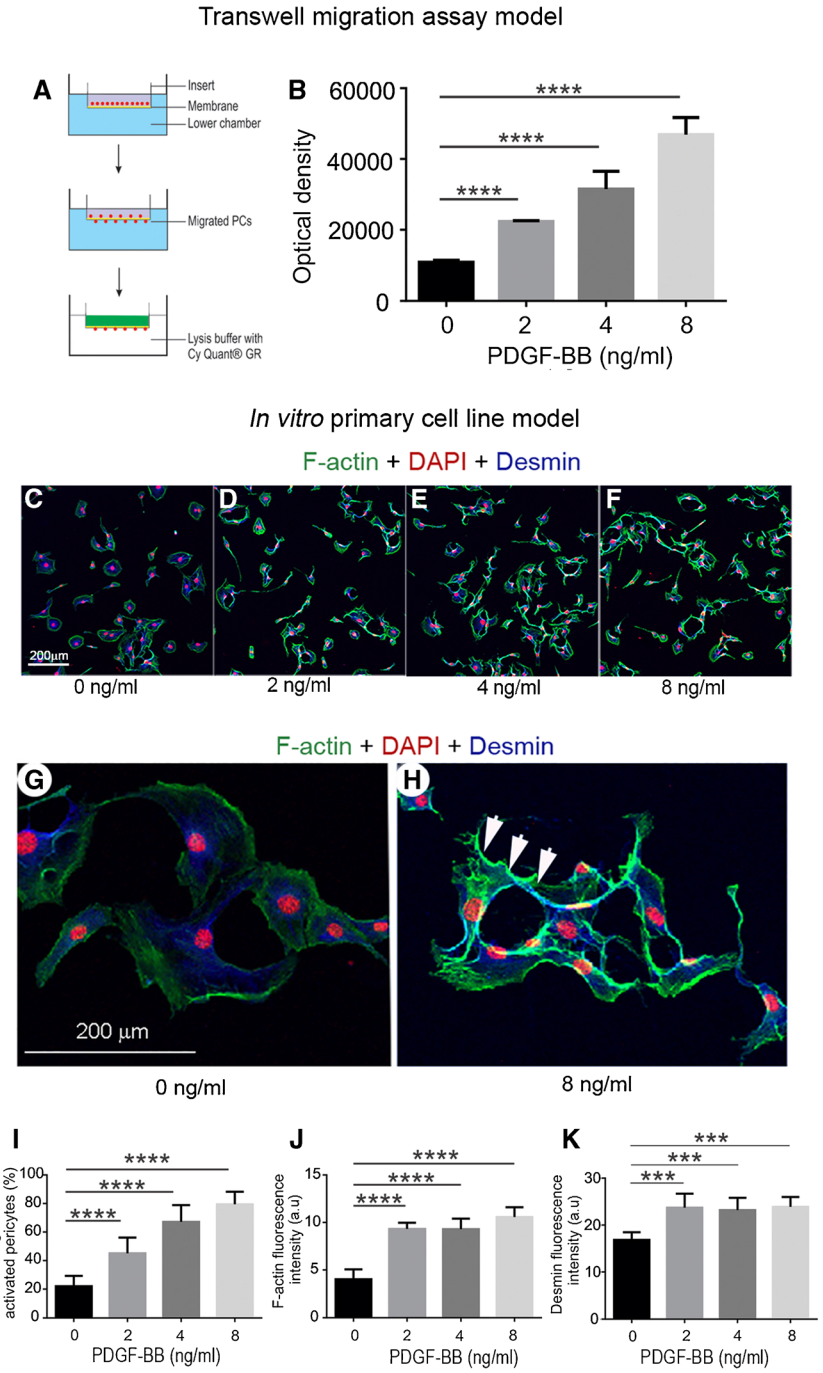

FIG. 3. PDGF-BB promotion of pericyte migration was confirmed in *in vitro* models. (A) PDGF-BB-induced pericyte migration was tested in a transwell cell migration assay. (B) The level of pericyte migration was highly associated with the level of PDGF-BB [$n = 6$, $F_{(3,\ 20)} = 112$, $^{****}P < 0.0001$, one-way ANOVA; $^{****}P$(2 ng/ml vs 0 ng/ml) < 0.0001, $^{****}P$(4 ng/ml vs 0 ng/ml) < 0.0001, $^{****}P$(8 ng/ml vs 0 ng/ml) < 0.0001] . (C–H) Pericytes were triple labeled with DAPI (red), Alexa 488 phalloidin for F-actin (green), and antibody specific for desmin (blue). Non-stimulated pericytes are large and flat with a fan-like morphology, as in (C). Stimulated pericytes are polarized with long, thin processes and relatively high fluorescence signal for F-actin, see also (D, E and F). (G and H) High magnification confocal projection images respectively show weak fluorescence signal for actin filaments in the non-stimulated pericytes (G) and increased fluorescence signal for F-actin filaments at the leading edge of cells stimulated by PDGF-BB (H, white arrows). (I–K) respectively show the degree of morphological change in pericytes [$n = 20$, $F_{(3,\ 54)} = 98.67$, $^{****}P < 0.0001$, one-way ANOVA; $^{****}P$(2 ng/ml vs 0 ng/ml) < 0.0001, $^{****}P$(4 ng/ml vs 0 ng/ml) < 0.0001, $^{****}P$(8 ng/ml vs 0 ng/ml) < 0.0001], and the fluorescence level of expression of F-actin [$n = 20$, $F_{(3,\ 20)} = 53.5$, $^{****}P < 0.0001$, one-way ANOVA; $^{****}P$(2 ng/ml vs 0 ng/ml) < 0.0001, $^{****}P$(4 ng/ml vs 0 ng/ml) < 0.0001, $^{****}P$(8 ng/ml vs 0 ng/ml) < 0.0001] and desmin [$n = 20$, $F_{(3,\ 20)} = 12.16$, $^{****}P < 0.0001$, one-way ANOVA; $^{***}P$(2 ng/ml vs 0 ng/ml) < 0.001, $^{***}P$(4 ng/ml vs 0 ng/ml < 0.001, *** P(8 ng/ml vs 0 ng/ml) < 0.001]

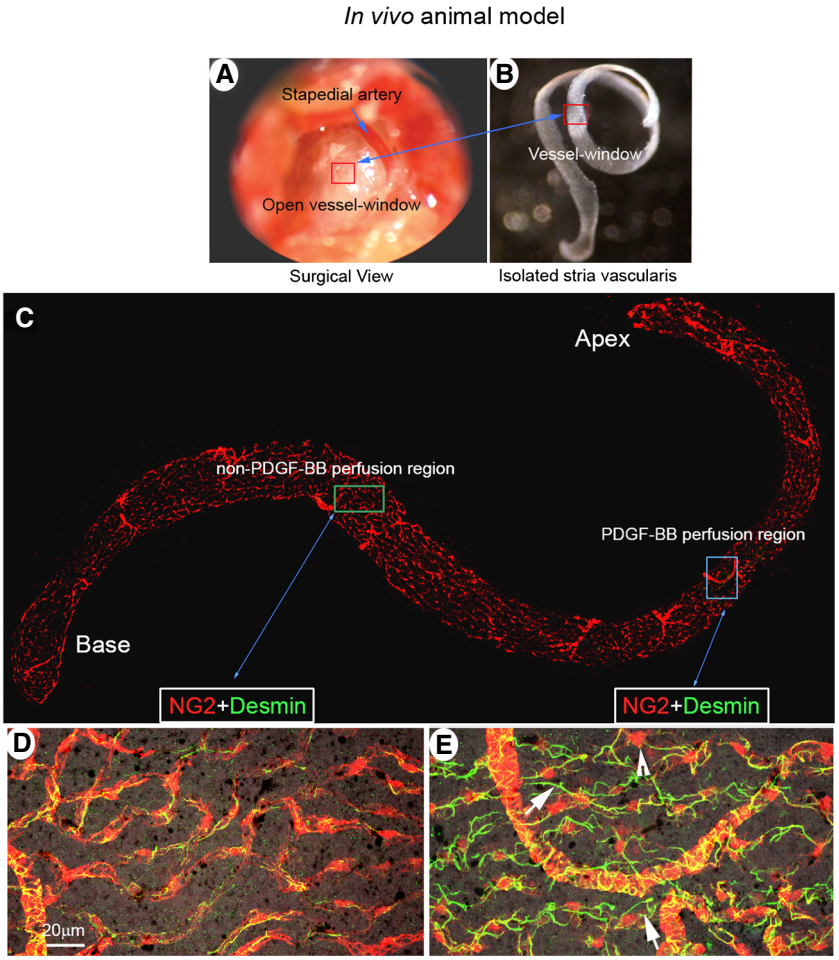

FIG. 4. PDGF-BB signaling induces pericyte migration in an in vivo animal model. (A) The red box indicates the location of the vessel-window created on the cochlear lateral wall. (B) shows the full-length of the stria vascularis isolated from a perfused mouse cochlea immediately after treatment. The red square indicates the location of the vessel-window. (C) The confocal projection image shows the post-fixed, full-length of the stria vascularis immunolabeled with desmin for visualization of pericyte processes. (D and E) are high magnification confocal projection images taken from non-PDGF-BB-perfused (green box in panel C) and PDGF-BB-perfused areas (blue box in panel C). In the non-PDGF-BB-perfused area pericytes tightly enshroud capillary walls. In contrast, in the PDGF-BB-perfused area, pericytes display irregularities, with retracted and detached foot processes (white arrows) and soma protrusion (white arrow head)

with microvillous protrusions in the pericyte-protruded region, as shown in Fig. 7(E) (purple box). Multiple vesicles are frequently seen in the endothelial cell and the pericyte is loosely attached (Fig. 7(F)). It is better visualized in the magnified image of panel (#) from region (#) of panel E and panel (*) from region (*) of panel F.

DISCUSSION

Normal hearing is dependent on the function of the microvasculature in the cochlea. Without proper blood supply and vascular integrity, the normal cochlear microenvironment is not maintained, increasing the likelihood of hearing loss. This study demonstrates that pericytes in the stria vascularis are highly sensitive and vulnerable to acoustic trauma. On exposure to loud sound, the pericytes protrude and detach from endothelial cells. PDGF-BB signaling mediates the protrusion and detachment. The pericyte migration caused vascular instability leads to regional vascular leakage. Our results demonstrate a new pericyte-related mechanism of noise-induced vascular damage in the ear. Targeting pericyte migration may help to control strial edema and restore tissue homeostasis in the stria vascularis.

THE PDGF-BB SIGNAL MEDIATES PERICYTE MIGRATION

Cell migration under pathological conditions is a typical response to adverse environmental stimuli, a

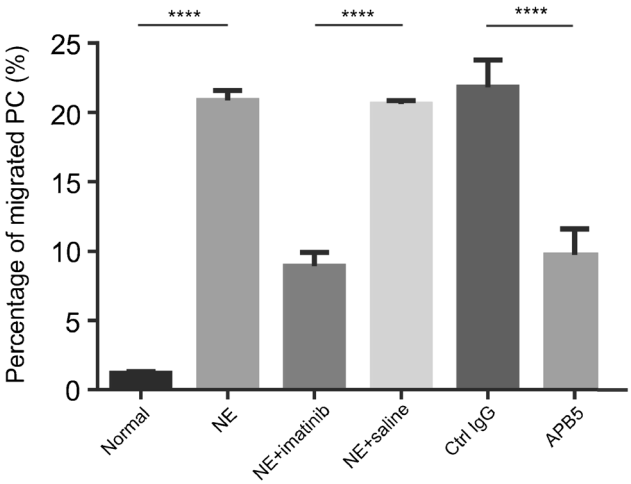

FIG. 5. Blocking PDGF-BB signaling significantly attenuates pericyte migration. The percentage of pericyte migration in loud sound-stimulated animals is higher than in control animals. However, pericyte migration can be significantly attenuated by pretreatment of the animals with imatinib, a potent PDGFRβ blocker, [$n_{ctrl} = 6$; $n_{lss} = 6$; $t\ (10) = 66.59$, $^{****}P_{(ctrl\ vs\ lss)} < 0.0001$, $n_{lss+imatinib} = 6$; $n_{lss+saline} = 6$; $t\ (10) = 118.6$, $^{****}P_{(lss+imatinib\ vs\ lss+saline)} < 0.0001$, Student's t test] or APB5, a specific blocker of PDGFRβ [$n_{lss+ctrl\ IgG} = 8$; $n_{lss+APB5} = 8$; $t\ (14) = 12.61$, $^{****}P_{(lss+ctrl\ IgG\ vs\ lss+APB5)} < 0.0001$, Student's t test]

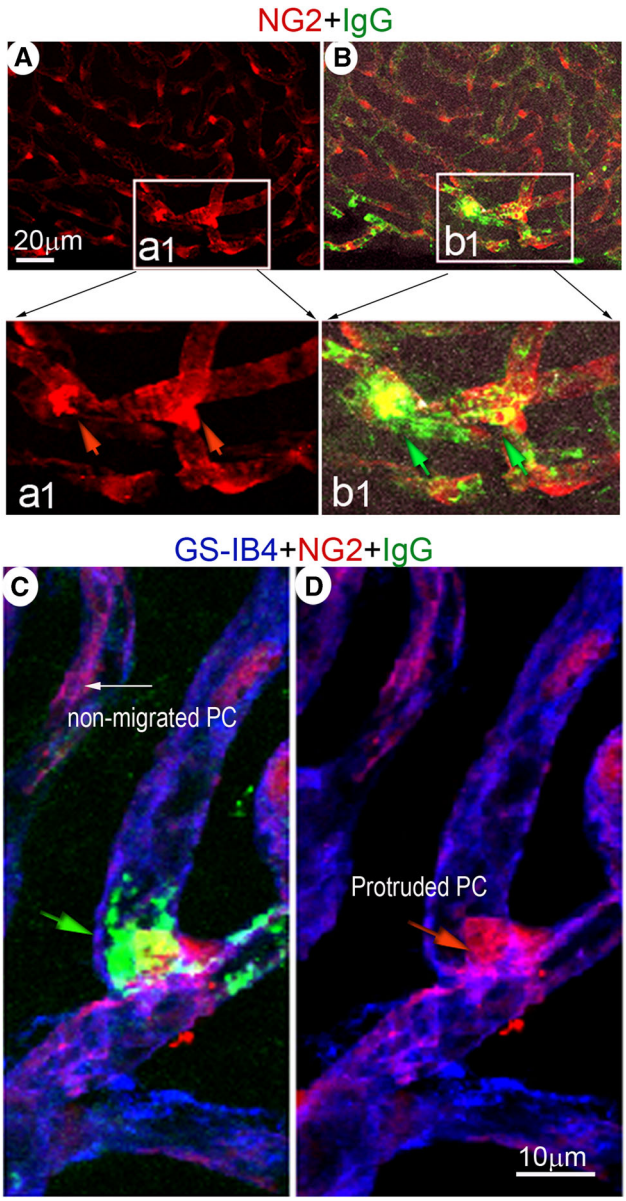

FIG. 6. IgG "site-leakage," assessed under confocal fluorescence microscopy, is preferentially observed at the site of pericyte protrusion. (A) A representative confocal projection image of whole mounted stria vascularis shows pericytes in a loud sound-stimulated animal. The square area (insert a1) highlights irregular and protruded pericytes. (B) is a merged image showing "localized" IgG leakage (green) near the site of morphologically irregular and protruded pericytes (insert b1). These features are better visualized in magnified image inserts a1 (red arrows point to protruded pericytes) and b1 (green arrows point to leaked IgG). (C) The confocal projection image shows "localized" leakage of IgG (green) from a vessel labeled with GS-IB4 (blue) in the vicinity of a protruded pericyte (red)

response which involves growth factors and cytokines (Yang et al. 2011). The signals and mechanisms governing pericyte migration are not yet fully identified. However, a number of studies have shown that platelet-derived growth factor (PDGF) plays an essential role in different types of cell migration, including pericyte migration (Facchiano et al. 2000; Sano et al. 2001; Sano et al. 2002; Hayashi et al. 2008; Armulik et al. 2010; Lentz et al. 2013; Shi et al. 2014; Zhang et al. 2015). In this study, we found that PDGF-BB is markedly upregulated at both the transcriptional and protein level immediately after acoustic trauma. The PDGF-BB receptor, PDGFRβ, is exclusively expressed on strial pericytes, and increased expression is seen in the migrated pericyte processes. Most importantly, blockade of the PDGF-BB receptor with either imatinib, a potent inhibitor of PDGFRα and PDGFRβ (Neng et al. 2013), or APB5, a specific PDGFRβ inhibitor (Sano et al. 2001; Sano et al. 2002; Hayashi et al. 2008), successfully attenuated pericyte protrusion and detachment in loud sound-traumatized animals. PDGF-BB directly induced migration of pericytes was also confirmed in other test models, including in a standard transwell cell migration assay and in *ex vivo* tissue and in vivo animal models.

The PDGF family consists of five different disulfide-bonded homo- and heterodimers: PDGF-AA, PDGF-AB, PDGF-BB, PDGF-CC, and PDGF-DD (Fredriksson et al. 2004). Among these forms, PDGF-BB is the most potent mediator for a number of cells, including smooth muscle cells and pericytes (Nadal et al. 2002; Niu et al. 2015; Kazlauskas 2017). For example, Zhang et al. (2015) recently demonstrated that PDGF-BB signal significantly

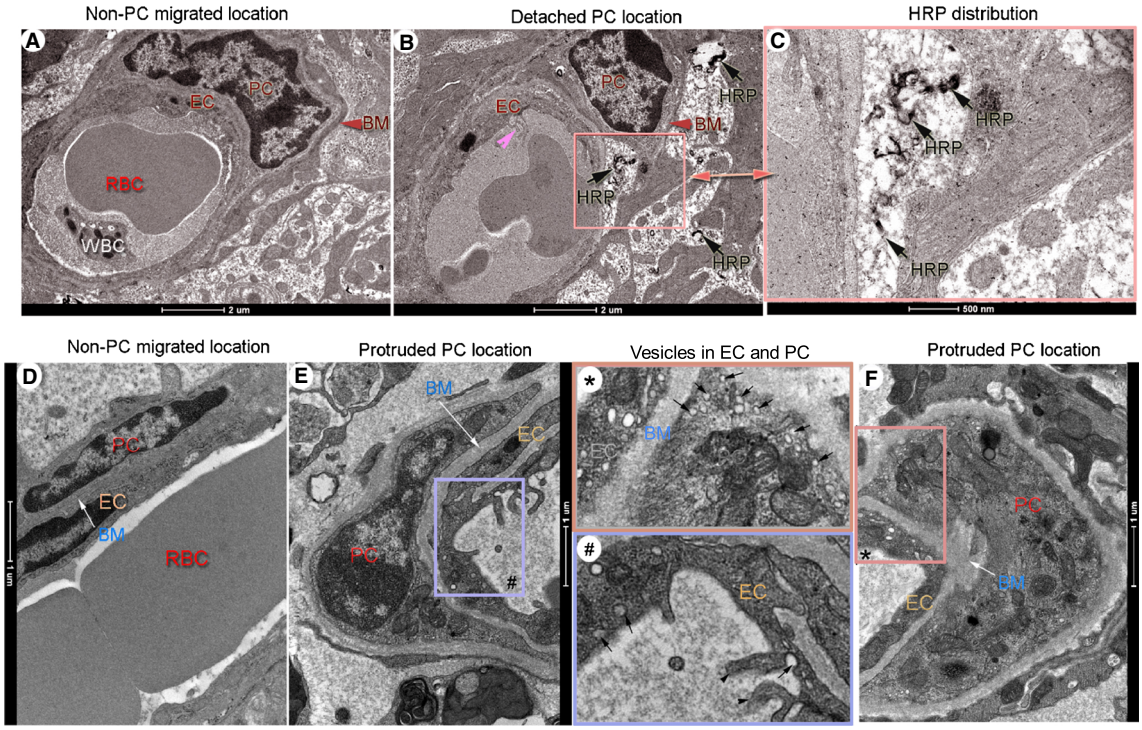

FIG. 7. Dark HRP signals are preferentially seen in areas of protruded and detached pericytes. (A–F) are representative TEM micrographs of horseradish peroxidase (HRP) distribution in non-migrated and migrated-pericyte locations in loud sound-exposed animals. (A) Electron micrographs of non-migrated pericytes are well sheathed within basement membrane and closely associated with a nearby endothelial cell. No detectable HRP signal is seen in the area after 30 min of HRP injection. (B) Dark HRP signals (black arrows) are seen in the vicinity of a detached pericyte soma (indicated by the pink square area in (B)). These are better seen under high magnification (C) from panel (B) (black arrows). (D) The cytoplasm of the endothelial cell is flattened and its luminal surface smooth in a non-migrated pericyte region. A dense basement membrane is situated between endothelial cell and pericyte (white arrow). (E) The luminal surface of the endothelial cell is undulated with microvillous protrusions (indicated by a purple box # in (E)) in a protruded pericyte region. (F) Multiple vesicles are seen at the sites of endothelial cells with loosely attached pericytes. These features are best seen in the high magnification images (**#**) from panel (E) and (*) from panel (F). Vesicles inside the endothelial cell and pericyte are indicated by the black arrows in the box * and box #. The luminal surface of the endothelial cell protrusion are indicated by the black arrowheads in the box **#**. EC: endothelial cells, PC: pericyte, BM: basement membrane, HRP: Horseradish peroxidase, RBC: red blood cell, WBC: white blood cell.

induces smooth muscle cell migration. Niu et al. (2015) showed PDGF-BB involved pericyte loss in human immunodeficiency virus infection. The exact mechanism by which PDGF-BB induces cochlear pericyte migration is not known. Studies in other tissues have shown that PDGF-BB binds to PDGFR-β, leading to non-covalent dimerization and auto-phosphorylation of the receptor on cytoplasmic tyrosine residues. The auto-phosphorylation of PDGFR-β consequently triggers downstream signaling, including in MAPK, ERK, JNK, p38 MAPK, and PI3K/Akt kinase pathways, causing rearrangement of the cytoskeleton, generation of locomotor force, and adhesion (Sano et al. 2001; Sano et al. 2002; Hayashi et al. 2008; Armulik et al. 2010; Zhang et al. 2015). This constellation of effects is necessary for cell protrusion (Graf et al. 1997; Zhang et al. 2015). In our study, we noticed that PDGF-BB induces remodeling of actin filaments in primary cultured pericytes (shown in Fig. 3). A marked increase in actin filaments is seen in the periphery of PDGF-BB-stimulated pericytes. The actin expression in the pericytes could be marking the internal forces leading to pericyte protrusion and detachment from the capillary wall.

Blockade of the PDGF-BB signal has shown effectiveness in reducing pericyte migration; however, we also note the pericyte migration is not fully stopped by blocking PDGF-BB activity. This is suggestive other signaling molecules are also involved in the pericyte migration. We previously reported that upregulation of VEGF following loud sound exposure is an important factor for increased expression of intermediate filament desmin in strial pericytes (Shi 2009). Others have also reported that VEGF acts as a pericyte mitogen under hypoxic conditions and that it stimulates migration of pericytes in a dose-dependent manner in cultivated bovine retinal pericytes (Yamagishi et al. 1999). Interestingly, a number of studies have shown VEGF-mediated cell migration also involves platelet-derived growth factor receptor-mediated tyrosine phosphorylation (Ball et al. 2007; Pennock et al.

2014). An early study (Nadal et al. 2002) showed other molecules such as angiotensin II also to stimulate migration of retinal microvascular pericytes. This migration involved both TGF-beta and PDGF-BB pathways. Collectively, these findings suggest the PDGF-BB signal may integrate or participate together with other molecules such as VEGF and angiotensin II to cause strial pericyte migration under pathological conditions. These conditions may include acoustic trauma in the ear. Our new results suggest increased levels of PDGF-BB strongly involved loud sound-induced strial pericyte migration. The findings provide evidence VEGF-induced upregulation of desmin following loud sound may be through a PDGF-BB-mediated pathway, as suggested in our earlier report.

Exactly how the PDGF-BB is upregulated is not clear. We suspect increased production of strial PDGF-BB under loud sound-stimulated conditions may be signaled through hypoxia-inducible factors (HIFs). Recent studies have demonstrated that HIF-1-alpha (HIF-1α), a transcription factor regulating expression of genes related to hypoxic stress, upregulates PDGF-BB (Schito et al. 2012; Li et al. 2015). For example, it has been shown that PDGF concentration is significantly increased under hypoxic conditions in the lungs of humans and mice with symptoms of pulmonary hypertension (Dahal et al. 2011). Previous studies, including ours, have shown that hypoxia in the ear after loud sound is immediate, and the effects persist after the loud sound is terminated (Graf et al. 1997; Niu et al. 2014). Induction of HIF-1α and its translocation is detected as early as 30 min after noise exposure (Chen et al. 2011). Is increased PDGF-BB production in the stria vascularis under loud sound conditions signaled by HIF-1α? In this report, we do not yet have the data to confirm this. The validity of this assumption virtually needs further investigation and verification.

INCREASED VASCULAR LEAKAGE PREFERENTIALLY OCCURS AT SITES OF PERICYTE MIGRATION

We found sites of pericyte migration highly associated with regions of vascular leakage. The pericytes are known to regulate microvascular permeability, development, and maturation by controlling endothelial cell functions (Sweeney et al. 2016). In general, pericytes form an umbrella-like cover over gaps between endothelial cells, holding extravasated cells and proteins within the vessel wall (Duz et al. 2007). Pericytes maintain vascular integrity by physically supporting vessel walls and by affecting formation of endothelial cell tight junctions (TJs), attenuating transcytosis in the endothelium, and depositing basement membrane (BM). Pericyte deficiency has been shown in other organs to result in increased vascular permeability, with corresponding disruption of TJs, defects in BM, and increased endothelial transcytosis (Jadeja et al. 2013; Hurtado-Alvarado et al. 2014; Lemos et al. 2016). In the ear, entry of serum proteins and inflammatory cells from leaky vessels, and tissue edema, has been frequently demonstrated in the acoustically traumatized cochlea (Suzuki et al. 2002; Hirose and Liberman 2003; Shi 2011; Zhang et al. 2013). However, in earlier studies it was not known vascular leakage is linked to pericyte migration. In the present study, we correlated the IgG leakage of capillary walls in the vicinity of migrating pericytes. We found leakage of plasma protein IgG "localized" largely to sites of pericyte protrusion or migration. We also observed the accumulation of HRP in the adjoining extracellular spaces of migrated pericytes, with the endothelial wall showing membranous inclusions and multiple vesicles in the endothelial cell. These findings indicate damaged endothelial cells and pericytes may cause weakening of the capillary wall, leading to regional "weak spots" or "abrupt breaks" in the blood-tissue barrier. Circulating sub-

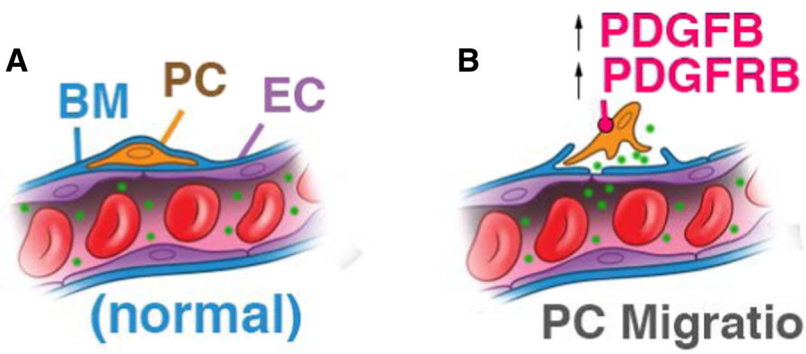

FIG. 8. An illustration of the mechanism of loud sound-induced pericyte migration in the cochlea. (A) Normal capillaries are composed of endothelial cells (ECs), with pericytes (PCs) embedded in basement membrane (BM). (B) Pericyte migration is mediated by increased PDGF-BB activity and vascular leakage occurs locally at sites of pericyte migration.

stances in the blood can then easily penetrate the broken blood-tissue barrier into the perivascular space. Our findings are in line with data from other labs which report pericytes critical for limiting vascular permeability (Lemos et al. 2016). Our finding is also in agreement with a recent report on human samples from Meniere's disease patients (Ishiyama et al. 2017) which show numerous vesicles within vascular endothelial cells where pericyte processes are detached and basement membrane is disrupted in the macula utricle. Our evidence also suggests increased transcytosis activity is a feature of increased vascular leakage. Taken together, our data show that abnormal interaction between pericytes and endothelium leads to increases in vascular extravasation. Pericyte migration is apparently a factor in the pathological event.

In conclusion, the integrity of the stria vascularis is known to be critical for maintaining the ionic and metabolic homeostasis required for normal hearing (Cohen-Salmon et al. 2007; Zhang et al. 2013; Chen et al. 2014a; Ingham et al. 2016; Shi 2016). Pericytes, as a mural component of the microvessel wall, are vital for structural and functional integrity. In this study, we found that pericytes are vulnerable and highly sensitive to acoustic trauma. Loud sound causes pericyte migration from capillary walls in the stria vascularis, and the migration is highly associated with PDGF-B signaling. Microvessels without intact pericytes are destabilized and this contributes to regional leakage (as illustrated in Fig. 8). Hearing acuity requires a healthy cochlear microenvironment, including normal functioning pericytes. These new findings suggest that targeting pericyte migration may open opportunities for new therapies for preventing early noise-induced tissue swelling and edema. Controlling tissue edema would provide a better ion microenvironment and increase cochlear oxygenation, and thus give injured sensory hair cells a better chance to survive by stabilizing them in late stage of loud sound stimulation, with the potential to improve hearing.

ACKNOWLEDGEMENTS

We would like to thank Drs. Neng Lingling and Wenjing Zhang (Oregon Hearing Research Center, Oregon Health and Science University) for their initial work in establishing a primary pericyte cell line from the stria vascularis in the Shi Lab. We also thank Dr. Alfred Nuttall (Oregon Hearing Research Center, Oregon Health and Science University) for his critical review and valuable discussion of the manuscript, Rachel Dumont Ph.D. for her assistance with the transmission electron microscopy, and Allan Kachelmeier B.S for his editing on this manuscript.

Funding Information This research was supported by NIH/NIDCD R21 DC016157 (X.Shi), NIH/NIDCD R01 DC015781 (X.Shi), NIH/NIDCD R01-DC010844 (X.Shi), NIH P30-DC005983 (Peter Barr-Gillespie), Medical Research Foundation from Oregon Health and Science University MRF (X.Shi), and P01GM051487-20 (Manfred Auer).

COMPLIANCE WITH ETHICAL STANDARDS

All authors have read and approved the manuscript.

All procedures in this study were reviewed and approved by the Institutional Animal Care and Use Committee (IACUC) at Oregon Health & Science University (IP 00000968).

Conflict of Interest The authors declare that they have no conflict of interest.

REFERENCES

Aguilera KY, Brekken RA (2014) Recruitment and retention: factors that affect pericyte migration. Cell Mol Life Sci 71:299–309

Armulik A, Genové G, Mäe M, Nisancioglu MH, Wallgard E, Niaudet C, He L, Norlin J, Lindblom P, Strittmatter K (2010) Pericytes regulate the blood-brain barrier. Nature 468:557–561

Ball SG, Shuttleworth CA, Kielty CM (2007) Vascular endothelial growth factor can signal through platelet-derived growth factor receptors. J Cell Biol 177:489–500

Bell RD, Winkler EA, Sagare AP, Singh I, Larue B, Deane R, Zlokovic BV (2010) Pericytes control key neurovascular functions and neuronal phenotype in the adult brain and during brain aging. Neuron 68:409–427

Chen YT, Chang FC, Wu CF, Chou YH, Hsu HL, Chiang WC, Shen J, Chen YM, Wu KD, Tsai TJ, Duffield JS, Lin SL (2011) Platelet-derived growth factor receptor signaling activates pericyte-myofibroblast transition in obstructive and post-ischemic kidney fibrosis. Kidney Int 80:1170–1181

Chen J, Ingham N, Kelly J, Jadeja S, Goulding D, Pass J, Mahajan VB, Tsang SH, Nijnik A, Jackson IJ, White JK, Forge A, Jagger D, Steel KP (2014a) Spinster homolog 2 (Spns2) deficiency causes early onset progressive hearing loss. PLoS Genet 10:E1004688

Chen Y, Teng X, Chen W, Yang J, Yang Z, Yu Y, Shen Z (2014b) Timing of transplantation of autologous bone marrow derived mesenchymal stem cells for treating myocardial infarction. Sci China Life Sci 57:195–200

Choudhury N, Chen F, Shi X, Nuttall AL, Wang RK (2009) Volumetric imaging of blood flow within cochlea in gerbil in vivo. IEEE J Sel Top Quantum Electron Pp:1–6

Cohen-Salmon M, Regnault B, Cayet N, Caille D, Demuth K, Hardelin JP, Janel N, Meda P, Petit C (2007) Connexin30 deficiency causes instrastrial fluid-blood barrier disruption within the cochlear stria vascularis. Proc Natl Acad Sci U S A 104:6229–6234

Dahal BK, Heuchel R, Pullamsetti SS, Wilhelm J, Ghofrani HA, Weissmann N, Seeger W, Grimminger F, Schermuly RT (2011) Hypoxic pulmonary hypertension in mice with constitutively active platelet-derived growth factor receptor-beta. Pulm Circ 1:259–268

Dai M, Shi X (2011) Fibro-vascular coupling in the control of cochlear blood flow. PLoS One 6:E20652

Devreotes P, Horwitz AR (2015) Signaling networks that regulate cell migration. Cold Spring Harb Perspect Biol 7:A005959

Donovan J, Abraham D, Norman J (2013) Platelet-derived growth factor signaling in mesenchymal cells. Front Biosci (Landmark Ed) 18:106–119

Dore-Duffy P, Owen C, Balabanov R, Murphy S, Beaumont T, Rafols JA (2000) Pericyte migration from the vascular wall in response to traumatic brain injury. Microvasc Res 60:55–69

Dore-Duffy P, Katychev A, Wang X, Van Buren E (2006) Cns microvascular pericytes exhibit multipotential stem cell activity. J Cereb Blood Flow Metab 26:613–624

Duz B, Oztas E, Erginay T, Erdogan E, Gonul E (2007) The effect of moderate hypothermia in acute ischemic stroke on pericyte migration: an ultrastructural study. Cryobiology 55:279–284

Facchiano A, De Marchis F, Turchetti E, Facchiano F, Guglielmi M, Denaro A, Palumbo R, Scoccianti M, Capogrossi MC (2000) The chemotactic and mitogenic effects of platelet-derived growth factor-bb on rat aorta smooth muscle cells are inhibited by basic fibroblast growth factor. J Cell Sci 113(Pt 16):2855–2863

Fredriksson L, Li H, Eriksson U (2004) The Pdgf family: four gene products form five dimeric isoforms. Cytokine Growth Factor Rev 15:197–204

Gonul E, Duz B, Kahraman S, Kayali H, Kubar A, Timurkaynak E (2002) Early pericyte response to brain hypoxia in cats: an ultrastructural study. Microvasc Res 64:116–119

Graf K, Xi XP, Yang D, Fleck E, Hsueh WA, Law RE (1997) Mitogen-activated protein kinase activation is involved in platelet-derived growth factor-directed migration by vascular smooth muscle cells. Hypertension 29:334–339

Gratton MA, Schmiedt RA, Schulte BA (1996) Age-related decreases in endocochlear potential are associated with vascular abnormalities in the stria vascularis. Hear Res 102:181–190

Greenhalgh SN, Iredale JP, Henderson NC (2013) Origins of fibrosis: pericytes take centre stage. F1000prime Rep 5. https://doi.org/10.12703/P5-37

Greenhalgh SN, Conroy KP, Henderson NC (2015) Healing scars: targeting pericytes to treat fibrosis. QJM 108:3–7

Greif DM, Eichmann A (2014) Vascular biology: brain vessels squeezed to death. Nature 508:50–51

Hall CN, Reynell C, Gesslein B, Hamilton NB, Mishra A, Sutherland BA, O'Farrell FM, Buchan AM, Lauritzen M, Attwell D (2014) Capillary pericytes regulate cerebral blood flow in health and disease. Nature 508:55–60

Hayashi H, Kunisada T, Takakura N, Aoki M, Mizuta K, Ito Y (2008) Involvement of platelet-derived growth factor receptor-B in maintenance of mesenchyme and sensory epithelium of the neonatal mouse inner ear. Hear Res 245:73–81

Hirose K, Liberman MC (2003) Lateral wall histopathology and endocochlear potential in the noise-damaged mouse cochlea. J Assoc Res Otolaryngol 4:339–352

Hurtado-Alvarado G, Cabanas-Morales AM, Gomez-Gonzalez B (2014) Pericytes: brain-immune Interface modulators. Front Integr Neurosci 7:80

Ingham NJ, Carlisle F, Pearson S, Lewis MA, Buniello A, Chen J, Isaacson RL, Pass J, White JK, Dawson SJ, Steel KP (2016) S1pr2 variants associated with auditory function in humans and endocochlear potential decline in mouse. Sci Rep 6:28964

Ishiyama G, Lopez IA, Ishiyama P, Vinters HV, Ishiyama A (2017) The blood labyrinthine barrier in the human normal and Meniere's disease macula utricle. Sci Rep 7:253

Jadeja S, Mort RL, Keighren M, Hart AW, Joynson R, Wells S, Potter PK, Jackson IJ (2013) A Cns-specific hypomorphic Pdgfr-beta mutant model of diabetic retinopathy. Invest Ophthalmol Vis Sci 54:3569–3578

Kazlauskas A (2017) Pdgfs and their receptors. Gene 614:1–7

Kim JM, Hong KS, Song WK, Bae D, Hwang IK, Kim JS, Chung HM (2016) Perivascular progenitor cells derived from human embryonic stem cells exhibit functional characteristics of pericytes and improve the retinal vasculature in a rodent model of diabetic retinopathy. Stem Cells Transl Med 5:1268–1276

Lemos DR, Marsh G, Huang A, Campanholle G, Aburatani T, Dang L, Gomez I, Fisher K, Ligresti G, Peti-Peterdi J, Duffield JS (2016) Maintenance of vascular integrity by pericytes is essential for normal kidney function. Am J Physiol Renal Physiol 311:F1230–F1242

Lentz JJ, Jodelka FM, Hinrich AJ, Mccaffrey KE, Farris HE, Spalitta MJ, Bazan NG, Duelli DM, Rigo F, Hastings ML (2013) Rescue of hearing and vestibular function by antisense oligonucleotides in a mouse model of human deafness. Nat Med 19:345–350

Li L, Xu M, Li X, Lv C, Zhang X, Yu H, Zhang M, Fu Y, Meng H, Zhou J (2015) Platelet-derived growth factor-B (Pdgf-B) induced by hypoxia promotes the survival of pulmonary arterial endothelial cells through the Pi3k/Akt/Stat3 pathway. Cell Physiol Biochem 35:441–451

Liu S, Agalliu D, Yu C, Fisher M (2012) The role of pericytes in blood-brain barrier function and stroke. Curr Pharm Des 18:3653–3662

Nadal JA, Scicli GM, Carbini LA, Scicli AG (2002) Angiotensin II stimulates migration of retinal microvascular pericytes: involvement of Tgf-beta and Pdgf-BB. Am J Physiol Heart Circ Physiol 282:H739–H748

Neng L, Zhang F, Kachelmeier A, Shi X (2013) Endothelial cell, pericyte, and perivascular resident macrophage-type melanocyte interactions regulate cochlear intrastrial fluid-blood barrier permeability. J Assoc Res Otolaryngol 14:175–185

Neng L, Zhang J, Yang J, Zhang F, Lopez IA, Dong M, Shi X (2015) Structural changes in thestrial blood-labyrinth barrier of aged C57bl/6 mice. Cell Tissue Res 361:685–696

Niu F, Yao H, Zhang W, Sutliff RL, Buch S (2014) Tat 101-mediated enhancement of brain pericyte migration involves platelet-derived growth factor subunit B homodimer: implications for human immunodeficiency virus-associated neurocognitive disorders. J Neurosci 34:11812–11825

Niu F, Yao H, Liao K, Buch S (2015) HIV Tat 101-mediated loss of pericytes at the blood-brain barrier involves PDGF-BB. Ther Targets Neurol Dis 2(1). https://doi.org/10.14800/ttnd.471

O'Farrell FM, Attwell D (2014) A role for pericytes in coronary no-reflow. Nat Rev Cardiol 11:427–432

Ohlemiller KK, Rice ME, Gagnon PM (2008) Strial microvascular pathology and age-associated endocochlear potential decline in nod congenic mice. Hear Res 244:85–97

Pennock S, Haddock LJ, Mukai S, Kazlauskas A (2014) Vascular endothelial growth factor acts primarily via platelet-derived growth factor receptor A to promote proliferative vitreoretinopathy. Am J Pathol 184:3052–3068

Peppiatt CM, Howarth C, Mobbs P, Attwell D (2006) Bidirectional control of Cns capillary diameter by pericytes. Nature 443:700–704

Pfister F, Feng Y, Vom Hagen F, Hoffmann S, Molema G, Hillebrands JL, Shani M, Deutsch U, Hammes HP (2008) Pericyte migration: a novel mechanism of pericyte loss in experimental diabetic retinopathy. Diabetes 57:2495–2502

Quaegebeur A, Segura I, Carmeliet P (2010) Pericytes: blood-brain barrier safeguards against neurodegeneration? Neuron 68:321–323

Salt AN, Melichar I, Thalmann R (1987) Mechanisms of endocochlear potential generation by stria vascularis. Laryngoscope 97:984–991

Sano H, Sudo T, Yokode M, Murayama T, Kataoka H, Takakura N, Nishikawa S, Nishikawa S-I, Kita T (2001) Functional blockade of platelet-derived growth factor receptor-B but not of receptor-A prevents vascular smooth muscle cell accumulation in fibrous cap lesions in apolipoprotein E–deficient mice. Circulation 103:2955–2960

Sano H, Ueda Y, Takakura N, Takemura G, Doi T, Kataoka H, Murayama T, Xu Y, Sudo T, Nishikawa S (2002) Blockade of

platelet-derived growth factor receptor-B pathway induces apoptosis of vascular endothelial cells and disrupts glomerular capillary formation in neonatal mice. Am J Pathol 161:135–143

Schito L, Rey S, Tafani M, Zhang H, Wong CC, Russo A, Russo MA, Semenza GL (2012) Hypoxia-inducible factor 1-dependent expression of platelet-derived growth factor B promotes lymphatic metastasis of hypoxic breast cancer cells. Proc Natl Acad Sci U S A 109:E2707–E2716

Shepro D, Morel NM (1993) Pericyte physiology. FASEB J 7:1031–1038

Shi X (2009) Cochlear pericyte responses to acoustic trauma and the involvement of hypoxia-inducible factor-1alpha and vascular endothelial growth factor. Am J Pathol 174:1692–1704

Shi X (2011) Physiopathology of the cochlear microcirculation. Hear Res 282:10–24

Shi X (2016) Pathophysiology of the cochlear intrastrial fluid-blood barrier (review). Hear Res 338:52–63

Shi X, Zhang F, Urdang Z, Dai M, Neng L, Zhang J, Chen S, Ramamoorthy S, Nuttall AL (2014) Thin and open vessel windows for intra-vital fluorescence imaging of murine cochlear blood flow. Hear Res 313:38–46

Sims DE (1986) The Pericyte—a review. Tissue Cell 18:153–174

Suzuki M, Yamasoba T, Ishibashi T, Miller JM, Kaga K (2002) Effect of noise exposure on blood-labyrinth barrier in Guinea pigs. Hear Res 164:12–18

Sweeney MD, Ayyadurai S, Zlokovic BV (2016) Pericytes of the neurovascular unit: key functions and signaling pathways. Nat Neurosci 19:771–783

Wangemann P (2002) Cochlear blood flow regulation. Adv Otorhinolaryngol 59:51–57.

Yamagishi S, Yonekura H, Yamamoto Y, Fujimori H, Sakurai S, Tanaka N, Yamamoto H (1999) Vascular endothelial growth factor acts as a pericyte mitogen under hypoxic conditions. Lab Investig 79:501–509

Yang Y, Dai M, Wilson TM, Omelchenko I, Klimek JE, Wilmarth PA, David LL, Nuttall AL, Gillespie PG, Shi X (2011) Na+/K+-Atpase Alpha1 identified as an abundant protein in the blood-labyrinth barrier that plays an essential role in the barrier integrity. PLoS One 6:E16547

Yoshida N, Liberman MC (1999) Stereociliary anomaly in the Guinea pig: effects of hair bundle rotation on cochlear sensitivity. Hear Res 131:29–38

Zhang W, Dai M, Fridberger A, Hassan A, Degagne J, Neng L, Zhang F, He W, Ren T, Trune D (2012) Perivascular-resident macrophage-like melanocytes in the inner ear are essential for the integrity of the intrastrial fluid–blood barrier. Proc Natl Acad Sci U S A 109:10388–10393

Zhang F, Dai M, Neng L, Zhang JH, Zhi Z, Fridberger A, Shi X (2013) Perivascular macrophage-like melanocyte responsiveness to acoustic trauma—a salient feature of strial barrier associated hearing loss. FASEB J 27:3730–3740

Zhang F, Hao F, An D, Zeng L, Wang Y, Xu X, Cui MZ (2015) The matricellular protein Cyr61 is a key mediator of platelet-derived growth factor-induced cell migration. J Biol Chem 290:8232–8242